

A 46% Efficient 0.8dBm Transmitter for Wireless Sensor Networks

Y. H. Chee, A. M. Niknejad, J. Rabaey

Berkeley Wireless Research Center, Dept. of EECS, University of California, Berkeley
2108 Allston Way, Suite 200, Berkeley, CA 94704, U.S.A.

Abstract – This paper presents a 1.9GHz low power transmitter for wireless sensor networks. It uses Film Bulk Acoustic Resonators (FBAR) for RF carrier generation and is co-designed with the antenna. The two-channel transmitter is 46% efficient when radiating 1.2mW from a 650mV supply. With 50% on-off keying, it consumes 1.35mW and supports data rate up till 330kbps. The 1.2x0.8mm² transmitter is implemented in 0.13μm CMOS and is integrated into a 38x25x8.5mm³ solar powered sensor node.

I. INTRODUCTION

Recent advances in RF MEMS and CMOS technology have made it conceivable to build a dense network of small and inexpensive wireless sensor nodes [1]. The key challenge to widespread deployment of wireless sensor network (WSN) is reducing the node's energy consumption, since it is infeasible to replace batteries of thousands of nodes. Typically, communication between nodes accounts for most of the power budget and hence, it is essential to have an energy efficient transmitter.

In WSN, the node distance is ≤ 10 m and the radiated power P_{rad} is ≤ 1 mW. At such low P_{rad} , the power dissipation of the circuits prior to the power amplifier $P_{\text{Pre-PA}}$ is significant and degrades the transmitter efficiency substantially. To achieve high efficiency at low P_{rad} , we propose a direct modulation transmitter using RF MEMS (FBAR) and PA-antenna co-design. Dual gain stages are also used during oscillator startup to reduce transmit time.

II. TRANSMITTER DESIGN

The 0.8dBm transmitter consists of two distinct FBAR oscillators to create two channels at 1.863GHz and 1.916GHz and a low power amplifier (LPA) co-designed with its antenna as shown in Fig. 1. Baseband data is modulated onto the carrier using on off keying (OOK) by power cycling the FBAR oscillator and the low power amplifier via its foot switch and gate bias respectively. With only one pre-PA circuit per channel, $P_{\text{Pre-PA}}$ is reduced significantly.

The Pierce oscillator uses a high Q FBAR [2] shown in Fig. 2 to reduce its power dissipation. The FBAR behaves like a capacitor except at resonance, where it has $Q > 1000$. Using CMOS amplifier halved the current consumption since the transistors share the same current while their g_m sum. To reduce the power consumption further, sub-threshold operation is employed for higher g_m/I_d . A large R_b is used to bias the transistors at $V_{\text{dd}}/2$ to maximize the voltage swing and minimize its loading on the FBAR. The 3-bits capacitor array C_1 allows adjustment of the oscillation frequency to mitigate process variations. For OOK modulation, the data rate is determined by the oscillator's startup time. To achieve

a higher data rate, an additional amplifier consisting of M_1 - M_2 is employed during startup.

The LPA is co-designed with the printed inverted L antenna (PILA) to eliminate losses in the matching network. The antenna provides an admittance of $(5-j17)\times 10^{-3} \Omega^{-1}$ which maximizes the LPA efficiency. The PILA antenna has an efficiency of 98% and an impedance bandwidth of ~ 300 MHz to mitigate manufacturing and environmental variations. To achieve the maximum TX efficiency, the LPA is co-designed with oscillator to achieve the optimal tradeoff between the LPA efficiency and its drive requirements.

III. WIRELESS SENSOR NODE

The transmitter is integrated into a solar powered sensor node as shown in Fig. 3. A regulator is used to charge two NiMH batteries, which in turn power the rest of the system. The node is equipped with sensors to measure temperature, humidity, acceleration and tilt. A low power microcontroller interfaces with the sensors and the transmitter. The sensors and transmitter are power gated to reduce standby power.

IV. IMPLEMENTATION AND RESULTS

The 1.2x0.8mm² transmitter is implemented in 0.13μm CMOS and is integrated with the FBAR resonators onto the sensor node using chip-on-board assembly as shown in Fig. 4. Two short bond wires are used to connect the FBAR to the CMOS die to avoid spurious oscillations. The node occupies 38x25x8.5 mm³ with the stacked solar cell.

Fig. 5 shows the transmitter efficiency and power consumption as a function of output power. The transmitter achieves a maximum efficiency of 46% while delivering 1.2mW and consumes 1.35mW with 50% OOK data. Fig. 6 shows the startup transient of the oscillator. By using dual amplifiers during start up, the start up time is reduced from 580ns to 300ns without significant increase in $P_{\text{Pre-PA}}$. This allows the transmitter to support a maximum data rate of 330kbps if the startup time equals to 10% of the symbol period. Due to the high Q FBAR, a clean and stable carrier is obtained. The measured phase noise is -106dBc/Hz at 10kHz offset and -124dBc/Hz at 100kHz offset. Fig. 7 shows the waveforms of the transmit sensor node. The microcontroller timer periodically wakes up the sensors/transmitter to collect the sensor data or transmit them before returning to sleep mode. In the sleep mode, the only the timer is active to minimize power consumption.

V. CONCLUSIONS

Using RF MEMS and PA-antenna co-design, a low power transmitter is implemented and integrated into a sensor node. Its performance compares favorably with other state-of-the-art transmitters as shown in Table 1.

ACKNOWLEDGEMENTS

The authors would like to thank Agilent Technologies and ST Microelectronics for the FBAR resonator and CMOS fabrication respectively. The authors also like to thank Rach Liu, Philip Liu and Fan Zhang for their assistance. This research was funded in part by DARPA (Grant No. N66001-01-1-8967).

REFERENCES

- [1] J. Rabaey, et al., *ISSCC Dig. Tech. papers*, pp. 200-201, Feb 02
- [2] R.C. Ruby, et. al., *Ultrasonics Symp Proc.*, pp. 813-821, Oct 01
- [3] Y. H. Chee, et. al., *CICC Proc.*, pp. 797-800, Sep. 05
- [4] B. Otis, et. al., *ISSCC Dig. Tech. papers*, pp. 396-397, Feb 02
- [5] A. Molnar, et. al., *CICC Proc.*, pp. 401-404, Oct. 04
- [6] P. Choi, et al., *ISSCC Dig. Tech. papers*, pp. 92-93, Feb 03

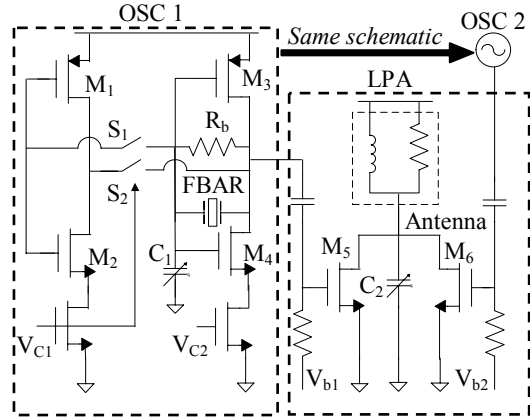


Fig. 1: Transmitter schematic

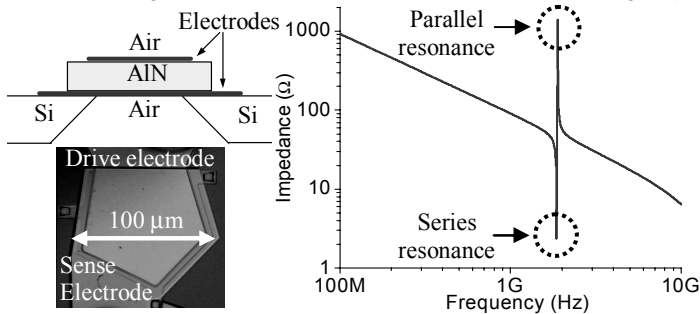


Fig. 2: Structure, die photo and frequency response of FBAR

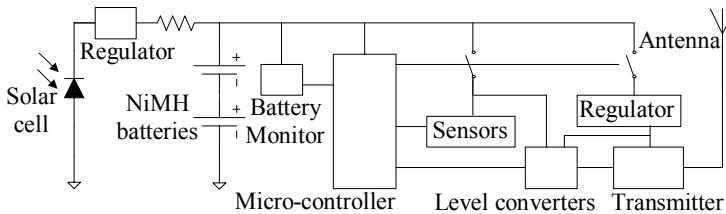


Fig. 3: Block diagram of transmit sensor node

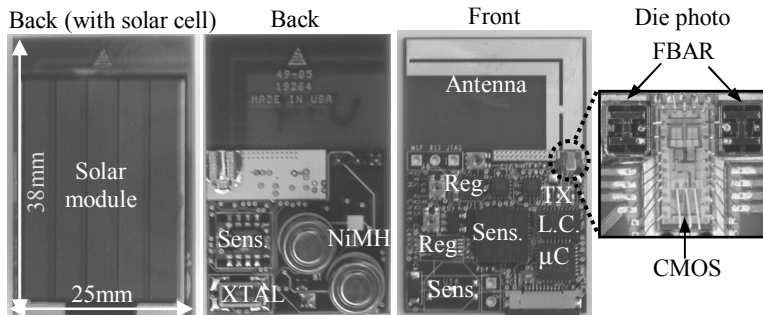


Fig 4: Wireless sensor node. Inset shows die photo

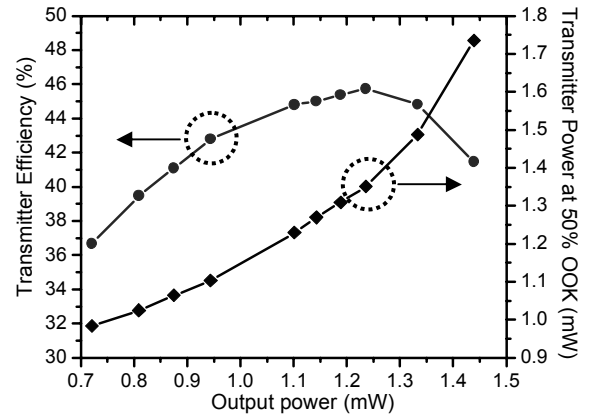


Fig. 5: Transmitter efficiency and power consumption

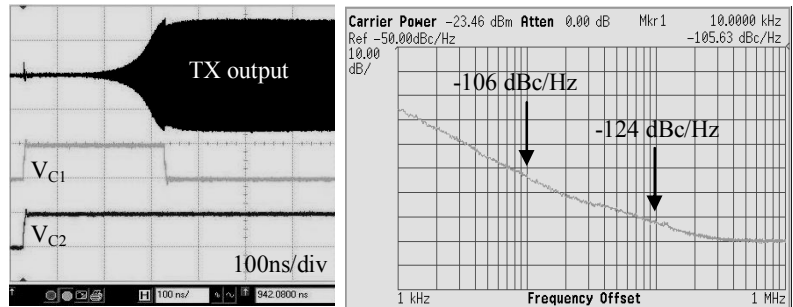


Fig 6: (left) Oscillator startup using dual amplifier and (right) phase noise

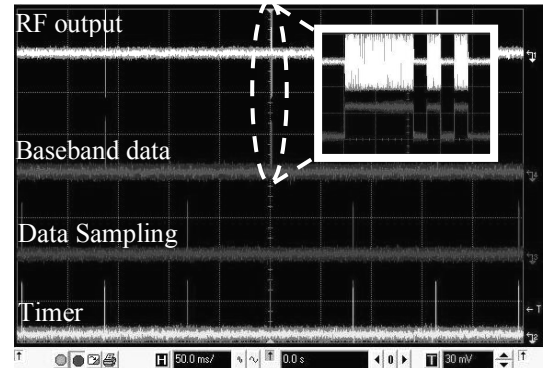


Fig. 7: Waveforms of transmit sensor node. Inset shows expanded RF output and baseband data waveforms.

Table 1: Performance comparison

Ref.	Freq GHz	Mod.	Data rate kbps	η_{TX} %	P_{rad} mW	P_{TX} mW	P_{ave} μW
This work	1.9	OOK	330	46	1.2	1.35	4.1
[3]	1.9	OOK	156	28	1	1.8	11
[4]	1.9	OOK	83	23	0.5	1.1	13
[5]	0.9	FSK	100	19	0.25	1.3	13
[6]	2.4	OQPSK	250	3.3	1	30	120

η_{TX} : TX efficiency when active

P_{TX} : TX power consumption. For OOK, assume equal probability of '1' and '0'

P_{rad} : Radiated power

P_{ave} : Average TX power with 1 packet/sec, 1000 bits/packet.